International Journal of Innovative Scientific & Engineering Technologies Research 14(3):206-223, July-Sept, 2026

© SEAHI PUBLICATIONS, 2026 www.seahipublications.org ISSN: 2360-896X

DOI:10.5281/zenodo.22877902

Implications Of Chemical Reaction In A Viscous Dissipative Fluid Affected By Velocity Slip, Thermal And Concentration Jump Conditions

Abdulsalam Shuaibu[1], Godwin Ojemeri[2*], Jeremiah Aaron Dazi[3], Haruna Ishaya Germache[4], Mustapha Khaleel-ullah Adeyemi[5] & Idris Omakwu Usman[6]

[1,2,3,4] Department of Mathematics,
College of Science,
Federal University of Agriculture, Zuru, Kebbi State, Nigeria

[5]Nigerian Institute of Leather and Science Technology, Zaria, Nigeria

[6]Brilliant Footsteps Academy International, Sokoto, Nigeria
***Corresponding Author's email: gojemeri.mth@fuaz.edu.ng, godwinojemeri@gmail.com**

ABSTRACT
A chemical reaction changes fluid composition and localized concentration gradients. By ignoring the reaction, models miscalculate the actual fluid velocity and shear stress profile near the wall. This makes it impossible to accurately assess how much the superhydrophobic slip actually reduces pumping power. Therefore, this study investigates the transport phenomena of a viscous incompressible fluid undergoing a homogeneous chemical reaction, utilizing non-linear velocity slip, thermal jump, and concentration jump boundary conditions. The governing is solved semi-analytically using regular perturbation method. Pertinent embedded parameters dictating the flow formation are graphically shown and discussed. The findings show that velocity slip reduces near-wall friction. At the same time, viscous dissipation coupled with thermal jumps significantly alters the chemical kinetic rate, necessitating these boundary considerations for accurate modeling in microfluidics, polymer processing, and hypersonic flows. Applications span micro-reactors, polymer extrusion, aerodynamic re-entry, and high-performance lubrication, with significance in improving computational fluid dynamics (CFD) accuracy by bridging macro- to micro-scale analysis. Comparison of results obtained in the present work for the limiting case with existing work demonstrates excellent agreement.
Keywords: Heat and Mass Transfer, Chemical Reaction, Viscous Dissipation, Velocity slip, Temperature jump, Concentration jump

1.0 INTRODUCTION
Several transport systems in industry and nature use buoyant force derived from thermal and mass diffusion, which is influenced by temperature and concentration variations between distinct chemical species. Temperature gradients and concentration differences drive these types of flows (Kaita *et al.* 2024). The study of steady/unsteady flows involving combined heat and mass transfer by free convection

with and without chemical reaction has been studied extensively by different researchers. Many chemical engineering processes, such as polymer production, manufacturing of ceramics or glassware, and food processing, may not be achieved when heat and mass transfer do not occur simultaneously. The phenomenon of heat and mass transfer is observed in buoyancy-induced motion in the atmosphere, water bodies, quasi-solid bodies such as the Earth, etc. The simultaneous occurrence of heat and mass transfer is of immense practical significance to engineers and scientists because of its almost universal incidence in many branches of science and engineering. Specifically, engineering applications like Nuclear power plants, missiles, gas turbines, and space vehicles, to mention a few, can benefit from this kind of fluid flow. To demonstrate the effects of heat and mass transfer in the presence of key physical parameters, Omokhuale and Ojemeri (2025) analyzed the magnetized heat and mass transfer flow of a viscous reactive fluid affected by symmetric wall concentration using a semi-analytical method. Saeed *et al.* (2019) discussed Heat and Mass transfer of free convection flow over a vertical plate with chemical reaction under the wall slip effect. Solutions for the fluid velocity, temperature, and concentration are achieved in closed form by applying the Laplace transform. Rout *et al.* (2013) established the MHD heat and mass transfer of chemical reaction fluid flow over a moving vertical plate in the presence of a heat source with convective surface boundary conditions. Sehra *et al.* (2021) studied convection heat mass transfer and MHD flow over a vertical plate with chemical reaction, arbitrary shear stress, and exponential heating. Sani and Kaita (2023) studied steady-state free convection with heat and mass transfer in the presence of variable thermal conductivity. Dagana and Amos (2020) investigated MHD free convection heat and mass transfer flow in a porous medium with Dufour and chemical reaction effects. Ajibade and Ojeagbase (2020) investigated steady natural convection heat and mass transfer flow through a vertical porous channel with viscosity and thermal conductivity. The variability in viscosity and thermal conductivity is considered as a linear function of temperature. Makinde (2010) investigated the effect of magnetized heat and mass transfer flow along an upward-stretching channel with Convective heating at the boundary. None of these works considered the impact of mixed convection in the presence of symmetric wall concentration and superhydrophobicity via microchannels.

The study of heat and mass transfer flow in the presence of chemical reactions has garnered a significant amount of interest due to its many practical uses in the chemical and hydrometallurgical industries. Homogeneous and heterogeneous chemical reactions are the two most common kinds of chemical reactions. If a chemical reaction takes place at an interface rather than in a single phase across its volume, it is referred to as a heterogeneous reaction rather than a homogeneous reaction. A heterogeneous reaction takes place in a confined area or inside the border of a phase, in contrast to a homogeneous reaction, which takes place evenly over the entire given phase. Melting, the production of ceramics and glassware, catalytic chemical reactors, the production of polymers, the manufacturing of ceramics and glassware, and the initiation of exothermic or endothermic chemical reactions are just some of the numerous important applications of heat and mass transfer flows with chemical reactions (Bafakeeh *et al*. 2022). Some researchers, mindful of the importance of this kind of study, have examined the hydromagnetic free-convection heat and mass-transfer flow of a viscous, incompressible, and electrically conducting fluid moving past a vertical plate in the presence of a first-order chemical reaction under a variety of conditions. The means by which a chemical reaction, with suction, might impact an isothermal moving vertical surface was investigated by Muthucumaraswamy (2002). Ajibade *et al.* (2016) discussed the impact of a chemical reaction on the erratic hydromagnetic natural convective Couette flow in a vertical channel packed with porous materials. Key authors like (Raghunath *et al.* 2021, Raghunath *et al.* 2022a, 2022b, Reddy *et al.* 2022, Ibrahim *et al.* 2008, Kesavaiah *et al.* 2011) investigated how different flow geometries are impacted by chemical interactions.

The development of microfluidic systems and advanced cooling technologies has increasingly relied on the manipulation of fluid flow and heat transfer at the microscale. Microfluidics has evolved immensely over the past decade as a consequence of its various applications in material manufacturing, micro-energy pipes, space technology, micro-jet boundary layer cooling, high-performance computing, high-power density transistors, and other devices. Because most of these simulations contain internal micro-channel

transport, a sound knowledge of the flow features has become critical for correct flow projections and conceptualization (Jha and Gwandu 2018, Jha *et al.* 2014). In this context, superhydrophobic surfaces that exhibit ultra-repellent properties have become highly relevant due to their ability to reduce drag and modify fluid dynamics in microchannels. Also, the study of heat transfer in superhydrophobic microchannels has garnered significant attention due to their potential applications in microfluidics, thermal management, and energy systems. Several outstanding scholars have greatly contributed to the studies of different effects in microchannels influenced by a superhydrophobic surface (SHS). In view of this, Ibrahim and Ojemeri (2026) recently semi-analytically studied the impact of a non-Newtonian fluid in a microchannel in the presence of viscous dissipation and a magnetic field effect. They concluded from their results that elevating the Jeffrey fluid parameter (which represents the viscoelasticity of the fluid) weakens the velocity gradient, as a result of the fluid resisting deformation more strongly on superhydrophobic surfaces. Hamza *et al.* (2026) investigated the influence of magnetized free flow in a viscous, dissipative, porous fluid in a slit microchannel using the regular perturbation method. Omokhuale *et al.* (2025) demonstrated how Arrhenius-controlled heat and mass transfer flow over a superhydrophobic microchannel with a uniform wall concentration is influenced by mixed convection under a constant pressure gradient. While the other parallel plate has a no-slip surface (NSS), one of the plates is purposefully altered to have a superhydrophobic surface (SHS). Hamza *et al.* (2024a, 2024b) reported the influence of electrokinetic effects on free and mixed convection flows in SHO microchannels and the temperature jump scenario. It is concluded from their computational analysis that the function of the SHS and electrokinetic effects is to enhance the fluid velocity in the microchannel. Ojemeri *et al*. (2024) explored the role of heat-generating/absorbing fluid on Arrhenius-controlled heat flow in an SHO-heated microchannel using a regular perturbation approach. Yale *et al.* (2023) discussed the consequences of super-hydrophobicity and MHD on a viscous dissipative fluid in a slit microchannel using a regular perturbation approach. Later on, Ojemeri and Onwubuya (2023) modified the work of Yale *et al.* (2023) to incorporate the effect of Darcy porous medium. They confirmed that due to the growth of the permeability of the porous medium, in the presence of superhydrophobic microchannel surface, the velocity gradient is observed increase drastically. Sharma *et al*. (2020) presented a mathematical model describing pressure-induced flow across a microchannel with textured SHS under constant heat flux. Other interesting research with different thermal boundary conditions in the presence of SHS can be seen in these references: Sia *et al.* 2023), Heidarian *et al.* (2020), and Zhang *et al*. (2019).

Although the mathematical model proposed by Ojemeri and Onwubuya (2023) examined the significance of a magnetic field and wall porosity in a viscous dissipative fluid using a superhydrophobic microchannel, their model contains fundamental knowledge gaps. Their study was strictly a hydrodynamic and thermal model. It omitted the species concentration equation and species buoyancy forces (solutal Grashof number). Also, the model featured no chemical reaction term (such as first-order or Arrhenius kinetics) within the fluid. That is, they assumed the fluid remained chemically inert. In real microfluidic chips, species undergo constructive or destructive chemical reactions. Without including a reaction parameter, the model could not account for how exothermic or endothermic chemical reactions alter fluid temperature, local viscosity, or concentration boundary layers. In view of the limitations found in the literature, the model of Ojemeri and Onwubuya (2023) is modified to incorporate mass transfer and chemical reactions. This upgraded model significantly bridges the gap between theoretical magnetohydrodynamics (MHD) and practical micro-engineering applications. Specifically, the presence of mass transfer introduces solutal buoyancy alongside thermal buoyancy. This dual-buoyancy mechanism (measured by the Grashof numbers) gives engineers a secondary lever to accelerate or decelerate the fluid without changing the temperature. Further, destructive chemical reactions decrease species concentration, which weakens the solutal buoyancy force. This leads to a predictable reduction in the overall fluid velocity across the microchannel.

2.0 Formulation of the Problem

Imagine an the electrically conducting fluid traveling gradually upward within a vertical parallel plate microchannel heated alternatively by wall constant temperature. Due to a particular micro-engineering

treatment, one of the surfaces is exceedingly difficult to wet (super-hydrophobic). The opposite wall (no-slip surface) was unaltered. As shown in Figure 1, the super-hydrophobic wall is kept at $y_0 = 0$, while the no-slip surface is kept at $y_0 = L$. Since the ultimate focus is on the superhydrophilicity of a surface rather than the flow behavior, various temperature jump and slip conditions were applied to opposite wall (no-slip surface) was unaltered. As shown in Figure 1, the super-hydrophobic wall is kept at $y_0 = 0$, while the no-slip surface is kept at $y_0 = L$. Since one of the key considerations in the present work is the presence of a superhydrophobic surface and the flow formation, various temperature jump and slip conditions were applied to the plates. equations

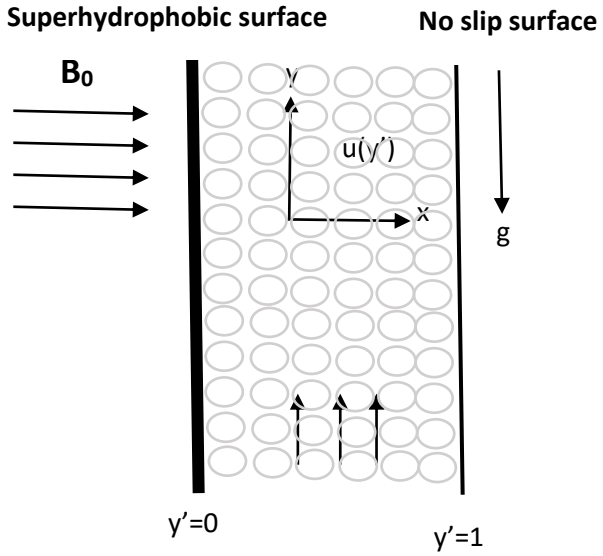

Figure 1: Flow Representation via a porous, superhydrophobic microchannel

According to Ojemeri and Onwubuya (2023) and employing the Boussisneq approximation, the dimensional governing for the present problem can be expressed as:

$$v\frac{d^2u'}{dy'^2} + g\beta_0(T' - T_O) + g\beta_1(C' - C_O) - \frac{\sigma B_0^2 u'}{\rho} - \frac{u'}{K} = 0 \tag{1}$$

$$\frac{k}{\rho c_\rho}\frac{d^2T'}{dy'^2} + \frac{v}{c_\rho}\left(\frac{du'}{dy'}\right)^2 = 0 \tag{2}$$

$$D\frac{d^2C'}{dy'^2} - K_r(C' - C_O) = 0 \tag{3}$$

Subject to the boundary conditions:

$$\left.\begin{aligned} u' &= \lambda'\frac{du'}{dy'},\ T' = T_w + \gamma'\frac{dT'}{dy'}, C' = C_w + \Gamma'\frac{dC'}{dy'} \ at\ y' = 0 \\ u' &= 0, \qquad T' = T_0, \qquad C' = C_0 \qquad at\ y' = H \end{aligned}\right\} \tag{4}$$

The dimensionless quantities and parameters employed are as follows:

$$u = \frac{u'}{U}, y = \frac{y'}{h}, T = \frac{T'-T_0}{T_w-T_0}, C = \frac{C'-C_0}{C_w-C_0},$$
$$M^2 = \frac{\sigma\beta_0^2 H^2}{\rho v}, Pr = \frac{v\rho c_p}{K}, Ec = \frac{u^2}{c_p(T_w-T_0)}, \quad U = \frac{v}{g\beta(T_w-T_0)H^2}, \mathrm{N} = \frac{g\beta^*(T_w-T_0)H^2}{vU}, \lambda = \frac{\lambda'}{H}, \gamma = \frac{\gamma'}{H}, \Gamma = \frac{\Gamma'}{H}$$
$$, K = \frac{k}{H^2}, K_r = \frac{\alpha^2 R_m}{v} \qquad (5)$$

Substituting eqn (5) into eqns (1) to (4), we have the basic equations as:

$$\frac{d^2U}{dy^2} - M_1^2 U + \theta + NC = 0 \qquad \text{s} \qquad (6)$$

$$\frac{d^2\theta}{dy^2} + Br\left(\frac{du}{dy}\right)^2 = 0 \qquad (7)$$

$$\frac{d^2C}{dy^2} - K_r C = 0 \qquad (8)$$

Where the boundary conditions are:

$$u(y) = \lambda\frac{du}{dy}; \quad \theta(y) = 1 + \gamma\frac{d\theta}{dy}; \quad C(y) = 1 + \Gamma\frac{dC}{dy}; \qquad \text{at } y = 0 \qquad (9)$$

$$u(y) = 0; \qquad \theta(y) = 0; \qquad C(y) = 0; \qquad \text{at } y = 1$$

Where $M_1^2 = M + \frac{1}{Da}$, Kr is the chemical reaction parameter, M is the magnetic parameter, Da is the Darcy porous medium, N is the sustentation parameter, Br = EcPr is the Brinkman number, λ is the velocity slip, and γ is the temperature jump parameter, and Γ is the concentration jump parameter.

3.0 Semi-analytical Solution

The coupled nonlinear governing equations are solved using the regular perturbation method, such that the solutions of the velocity, temperature, and concentration are assumed as;

$$U = u_0 + \mathrm{Br}(u_1) \qquad (10)$$

$$\theta = \theta_0 + \mathrm{Br}(\theta_1) \qquad (11)$$

$$C = F_0 + \mathrm{Br}(F_1) \qquad (12)$$

Inserting eqns (10) to (12) into eqns (6) to (9), and taking the coefficients of Br^0 and Br, we derive the following system of ordinary differential equations with their corresponding boundary conditions as:

$$\mathrm{Br}^0: \frac{d^2u_0}{dy^2} - M_1^2 u_0 + \theta_0 + Nc_0 = 0 \qquad (13)$$

$$\mathrm{Br}: \frac{d^2u_1}{dy^2} - M_1^2 u_1 + \theta_1 + Nc_1 = 0 \qquad (14)$$

$$\mathrm{Br}^0: \frac{d^2\theta_0}{dy^2} = 0 \qquad (15)$$

$$\mathrm{Br}: \frac{d^2\theta_1}{dy^2} + \left[\frac{du_0}{dy}\right]^2 = 0 \tag{16}$$

$$\mathrm{Br}^0: \frac{d^2c_0}{dy^2} - K_r c_0 = 0 \tag{17}$$

$$\mathrm{Br}: \frac{d^2c_1}{dy^2} - K_r c_1 = 0 \tag{18}$$

$$\left.\begin{aligned} \mathrm{Br}^0: u_0 &= \lambda \frac{dU_o}{dy} \\ \mathrm{Br}: u_1 &= \lambda \frac{dU_1}{dy} \\ \mathrm{Br}^0: \theta_o &= 1 + \gamma \frac{d\theta_o}{dy} \\ \mathrm{Br}: \theta_1 &= \gamma \frac{d\theta_1}{dy} \\ \mathrm{Br}^0: c_o &= 1 + \Gamma \frac{dc_o}{dy} \\ \mathrm{Br}: c_1 &= \Gamma \frac{dc_1}{dy} \end{aligned}\right\} \text{at } y = 0 \tag{19}$$

and

$$\left.\begin{aligned} \mathrm{Br}^0: u_0 &= 0 \\ \mathrm{Br}: u_1 &= 0 \\ \mathrm{Br}^0: \theta_0 &= 0 \\ \mathrm{Br}: \theta_1 &= 0 \\ \mathrm{Br}^0: c_0 &= 0 \\ \mathrm{Br}: c_1 &= 0 \end{aligned}\right\} \text{at } y = 1 \tag{20}$$

The solutions of $u_0, u_1, \theta_0, \theta_1, F_0, F_1$ have been obtained as follows

$$u_0 = D_1 e^{s_3 y} + D_2 e^{-s_4 y} + D_5 e^{s_1 y} + D_6 e^{-s_2 y} + D_3 y + D_4 \tag{21}$$

$$u_1 = D_7 e^{s_3 y} + D_8 e^{-s_4 y} + D_9 e^{2s_3 y} + D_{10} e^{(s_3 - s_4)y} + D_{11} e^{s_3 y} + D_{12} e^{(s_1 + s_3)y} + D_{13} e^{(s_3 - s_2)y} + D_{14} e^{-2s_4 y} + D_{15} e^{-s_4 y} + D_{16} e^{(s_1 - s_4)y} + D_{17} e^{-(s_2 + s_4)y} + D_{18} y^2 + D_{19} e^{s_1 y} + D_{20} e^{-s_2 y} + D_{21} e^{2s_1 y} + D_{22} e^{(s_1 - s_2)y} + D_{23} e^{-2s_2 y} + D_{24} y + D_{25} \tag{22}$$

$$\theta_0 = E_1 y + E_2 \tag{23}$$

$$\theta_1 = n_{31}e^{2s_3y} + n_{32}e^{(s_3-s_4)y} + n_{33}e^{s_3y} + n_{34}e^{(s_1+s_3)y} + n_{35}e^{(s_3-s_2)y} + n_{36}e^{2s_4y} + n_{37}e^{-s_4y} + n_{38}e^{(s_1-s_4)y} + n_{39}e^{-(s_2+s_4)y} + n_{40}y^2 + n_{41}e^{s_1y} + n_{42}e^{-s_2y} + n_{43}e^{2s_1y} + n_{44}e^{(s_1-s_2)y} + n_{45}e^{-2s_2y} + E_3y + E_4 \quad (24)$$

$$c_0 = F_1e^{s_1y} + F_2e^{-s_2y} \quad (25)$$

$$c_1 = 0 \quad (26)$$

Substituting eqns (21) and (22) into eqn (10), we have that

$$U = D_1e^{s_3y} + D_2e^{-s_4y} + D_5e^{s_1y} + D_6e^{-s_2y} + D_3y + D_4 + Br\left[D_7e^{s_3y} + D_8e^{-s_4y} + D_9e^{2s_3y} + D_{10}e^{(s_3-s_4)y} + D_{11}e^{s_3y} + D_{12}e^{(s_1+s_3)y} + D_{13}e^{(s_3-s_2)y} + D_{14}e^{-2s_4y} + D_{15}e^{-s_4y} + D_{16}e^{(s_1-s_4)y} + D_{17}e^{-(s_2+s_4)y} + D_{18}y^2 + D_{19}e^{s_1y} + D_{20}e^{-s_2y} + D_{21}e^{2s_1y} + D_{22}e^{(s_1-s_2)y} + D_{23}e^{-2s_2y} + D_{24}y + D_{25}\right] \quad (27)$$

Similarly, substituting eqns (23) ans (24) into eqn (11), and eqns (25) and (26) into eqn (12), we have that

$$\theta = E_1y + E_2 + Br\left[n_{31}e^{2s_3y} + n_{32}e^{(s_3-s_4)y} + n_{33}e^{s_3y} + n_{34}e^{(s_1+s_3)y} + n_{35}e^{(s_3-s_2)y} + n_{36}e^{2s_4y} + n_{37}e^{-s_4y} + n_{38}e^{(s_1-s_4)y} + n_{39}e^{-(s_2+s_4)y} + n_{40}y^2 + n_{41}e^{s_1y} + n_{42}e^{-s_2y} + n_{43}e^{2s_1y} + n_{44}e^{(s_1-s_2)y} + n_{45}e^{-2s_2y} + E_3y + E_4\right] \quad (28)$$

$$C = F_1e^{s_1y} + F_2e^{-s_2y} \quad (29)$$

Where the skin friction, Nusselt number and Sherwood number has been calculated as:

$$\frac{dU}{dy}\Big|_{y=0} = e^{s_3}D_1 - e^{-s_4}D_2 + e^{s_1}D_5 - e^{-s_2}D_6 + D_3 + Br[s_3D_7 - s_4D_8 + 2s_3D_9 + (s_3 - s_4)D_{10} + s_3D_{11} + (s_1 + s_3)D_{12} + (s_3 - s_2)D_{13} - 2s_4D_{14} - s_4D_{15} + (s_1 - s_4)D_{16} - (s_2 + s_4)D_{17} + s_1D_{19} - s_2D_{20} + 2s_1D_{21} + (s_1 - s_2)D_{22} - 2s_2D_{23} + D_{24}] \quad (30)$$

$$\frac{dU}{dy}\Big|_{y=1} = s_3D_1e^{s_3} - s_4D_2e^{-s_4} + s_1D_5e^{s_1} - s_2D_6e^{-s_2} + D_3 + Br\left[s_3D_7e^{s_3} - s_4D_8e^{-s_4} + 2s_3D_9e^{2s_3} + (s_3 - s_4)D_{10}e^{(s_3-s_4)} + s_3D_{11}e^{s_3} + (s_1 + s_3)D_{12}e^{(s_1+s_3)} + (s_3 - s_2)D_{13}e^{(s_3-s_2)} - 2s_4D_{14}e^{-2s_4} - s_4D_{15}e^{-s_4} + (s_1 - s_4)D_{16}e^{(s_1-s_4)} - (s_2 + s_4)D_{17}e^{-(s_2+s_4)} + 2D_{18} + s_1D_{19}e^{s_1} - s_2D_{20}e^{-s_2} + 2s_1D_{21}e^{2s_1} + (s_1 - s_2)D_{22}e^{(s_1-s_2)} - 2s_2D_{23}e^{-2s_2} + D_{24}\right] \quad (31)$$

$$\frac{d\theta}{dy}\Big|_{y=0} = E_1 + Br[2s_3n_{31} + (s_3 - s_4)n_{32} + s_3n_{33} + (s_1 + s_3)n_{34} + (s_3 - s_2)n_{35} + 2s_4n_{36} - s_4n_{37} + (s_1 - s_4)n_{38} + (s_2 + s_4)n_{39} + s_1n_{41} - s_2n_{42} + 2s_1n_{43} + (s_1 - s_2)n_{44} - 2s_2n_{45} + E_3] \quad (32)$$

$$\frac{d\theta}{dy}\Big|_{y=1} = E_1 + Br\big[2s_3n_{31}e^{2s_3} + (s_3 - s_4)n_{32}e^{(s_3-s_4)} + s_3n_{33}e^{s_3} + (s_1 + s_3)n_{34}e^{(s_1+s_3)} + (s_3 - s_2)n_{35}e^{(s_3-s_2)} + 2s_4n_{36}e^{2s_4} - s_4n_{37}e^{-s_4} + (s_1 - s_4)n_{38}e^{(s_1-s_4)} + (s_2 + s_4)n_{39}e^{-(s_2+s_4)} + 2n_{40} + s_1n_{41}e^{s_1} - s_2n_{42}e^{-s_2} + 2s_1n_{43}e^{2s_1} + (s_1 - s_2)n_{44}e^{(s_1-s_2)} - 2s_2n_{45}e^{-2s_2} + E_3\big] \quad (33)$$

$$\frac{dC}{dy}\Big|_{y=0} = s_1F_1 - s_2F_2 \quad (34)$$

$$\frac{dC}{dy}\Big|_{y=1} = s_1F_1e^{s_1} - s_2F_2e^{-s_2} \quad (35)$$

Due to the lengthiness of the constants used in this semi-analytical solution, the appendix will be available on request

4.0 RESULTS AND DISCUSSION

To see the effects of key physical parameters dictating the flow formation, illustrative graphs are plotted to describe these effects. Pertinent parameters under consideration include the chemical reaction parameter, K_r, Sustentation parameter, N, velocity slip parameter, λ, temperature jump parameter, γ, Concentration jump parameter, Γ, Darcy porous medium, Da, Magnetic parameter, M, and the Brinkman number, Br. The default values selected for this study are ($K_r = 0.5, N = 1, \lambda = \gamma = \Gamma = 1$, M=1.5, and Br= 0.001).

Figure 2 shows the impact of the chemical reaction parameter on the concentration gradient. Increasing the chemical reaction parameter causes the concentration profile to drop and become thinner. The reaction consumes the chemical species faster than diffusion can replenish it, lowering the concentration boundary layer thickness. Figure 3 displays the effect of the chemical reaction parameter on the velocity gradient. For destructive reactions, a higher reaction rate leads to a decrease in the fluid velocity profile. The chemical reaction consumes species and changes the buoyancy forces or species concentration gradients that drive fluid motion, resulting in a dampening effect on momentum transport and a thinner velocity boundary layer.

Figures 4 and 5 show the effect of γ_2 on the concentration and velocity profiles. A concentration jump increases the resistance between the fluid and its boundary layer. Increasing the interfacial barrier to mass transfer γ_2 reduces both the mass transfer coefficient and fluid velocity. In mass transfer, a concentration jump is a change in concentration at the interface between two phases. This effect is most noticeable when one phase has extremely poor solubility for the solute. This phenomenon is also used to assess whether gas-film or liquid-film resistance dominates transport in cells and in surface response modeling.

Figure 6 explains the behavior of N on the velocity distribution. The sustentation parameter or buoyancy term represents gravitational acceleration acting on density variations. Additionally, due to the gravitational interaction that acts on these density differences, a vertical or downward force is created that dictates the fluid movement. Buoyancy forces act as a momentum source or sink in the velocity equation. This phenomenon strongly affects heat and mass transfer rates. Outcomes of this study are relevant in real-world applications such as atmospheric and oceanic flows, cooling of electronic components, and various manufacturing processes involving heat treatment or material processing.

Figure 7 is plotted to demonstrate the influence of the Darcy porous medium on the fluid velocity. Higher Darcy numbers (representing greater permeability) increase fluid motion and raise local velocity values. The value of the Darcy number changes how much resistance the solid framework puts on the fluid. A high Darcy Number means that the material is highly porous with very little solid restriction. The velocity

profile behaves like a free fluid. In a pipe or channel, this means the velocity returns to a classic, curved parabolic profile with a fast peak in the center. The Darcy number is highly significant in physics and engineering because it acts as a flow-regime separator**.** Figure 8 depicts the fluid motion pattern as a function of the magnetic parameter M. The flow pattern clearly shows a reduction for all investigated M values. The existence of a magnetic effect causes this behavior by creating a resistive force (the Lorentz force) that restrains movement.

Figures 9 and 10 show the effect of viscous dissipation, Br, on steady temperature and velocity gradients. Since the Eckert number emanates from the kinetic energy of flow and heat enthalpy changes, an increase in the Eckert number promotes the kinetic energy. Consequently, higher viscous dissipative factors boost the fluid's temperature and velocity, respectively. Again, it is true that rising levels of the Brickman number represent better convective heating at the channel surface, leading to higher temperature and velocity at the plate surfaces. Figure 11(a and b) is sketched to describe the effect of varying a chemical reaction parameter on the skin friction for the lower and upper walls. When a chemical reaction consumes species in the boundary layer, the reaction dampens fluid velocity profiles. Because wall velocity gradients become less steep, skin friction decreases. Consuming the species faster steepens the concentration gradient at the wall. A sharper concentration gradient accelerates mass transfer, causing the Sherwood number to increase as shown in Figure 12 (a and b) for both boundary walls**.** Figure 13 displays the impact of N on the skin friction. Stronger values of N promote the shear stress in the microchannel at both walls.

In general, the study of a destructive (consuming) chemical reaction on a viscous dissipative fluid moving through a superhydrophobic microchannel helps engineers control how heat, mass, and fluids move in tiny devices. A destructive reaction slows the fluid down. Conversely, viscous dissipation heats the fluid up and thins it out, making it move faster. Balancing these forces allows engineers to precisely tune fluid speeds in tiny chips. Additionally, microfluidic chips used for blood testing or DNA mapping rely heavily on these mechanics. Superhydrophobic channels ensure biomolecules don't stick to the walls and cause clogging. Meanwhile, the consuming chemical reaction is used to clean up or neutralize hazardous bio-samples after testing.

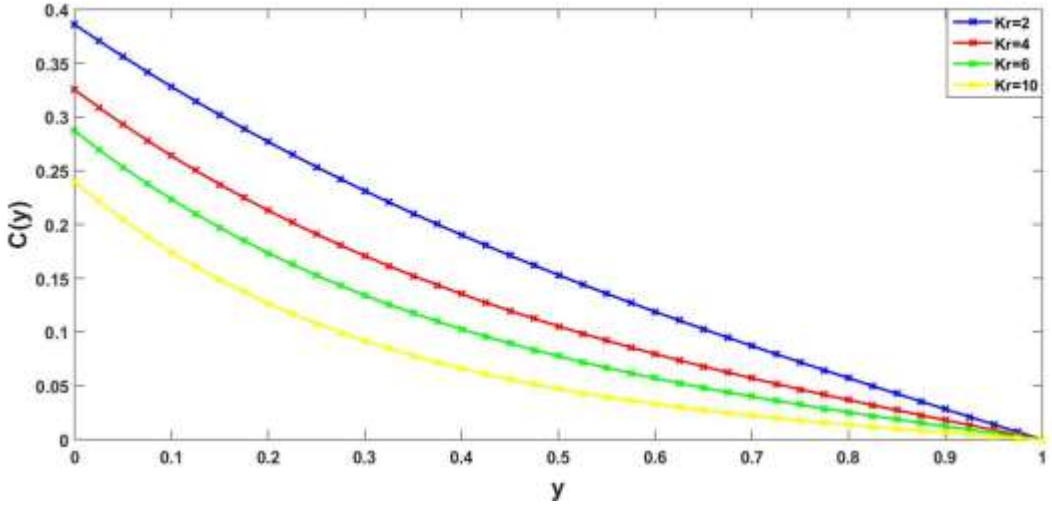

Figure 2: Concentration Changes for Chemical Reaction Parameter

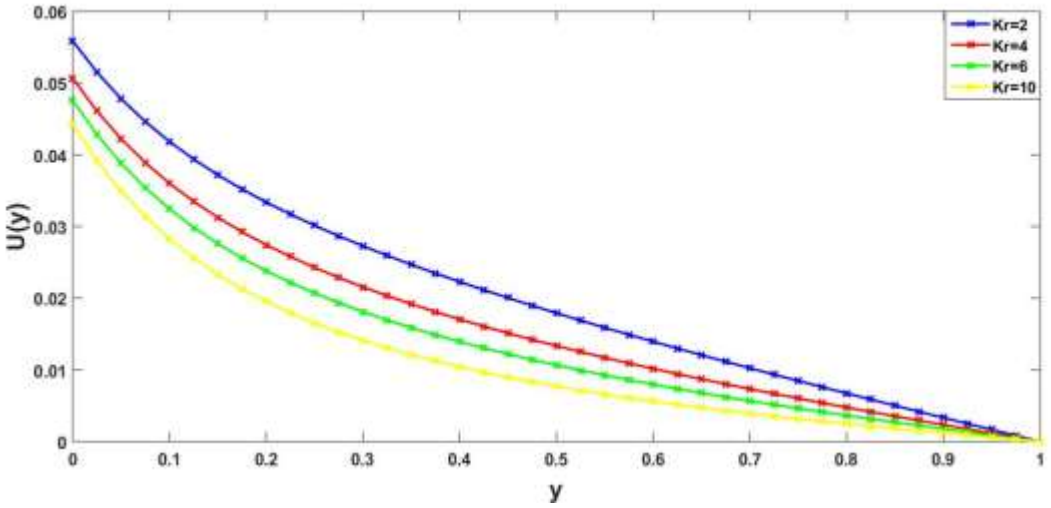

Figure 3: Velocity Changes for Chemical Reaction Parameter

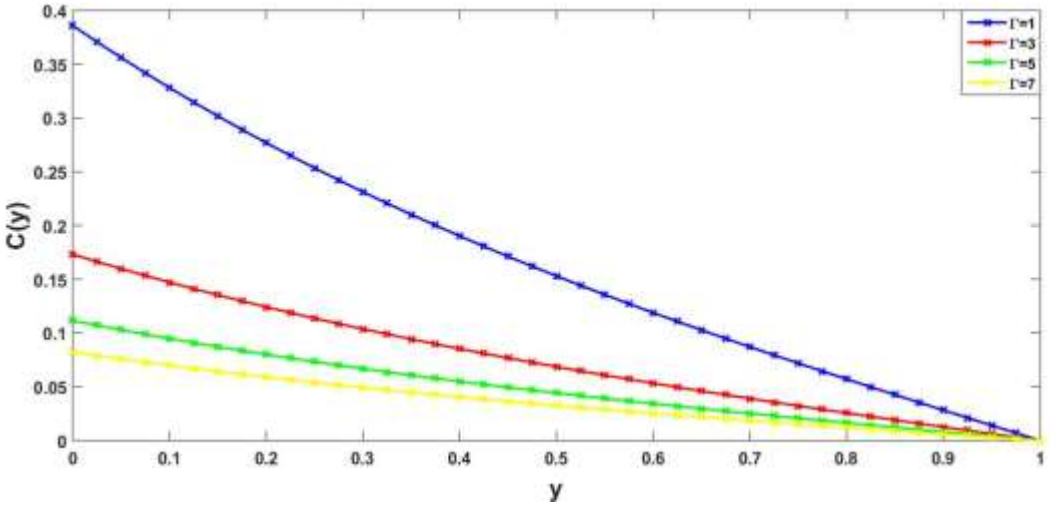

Figure 4: Concentration Changes for Concentration jump Parameter

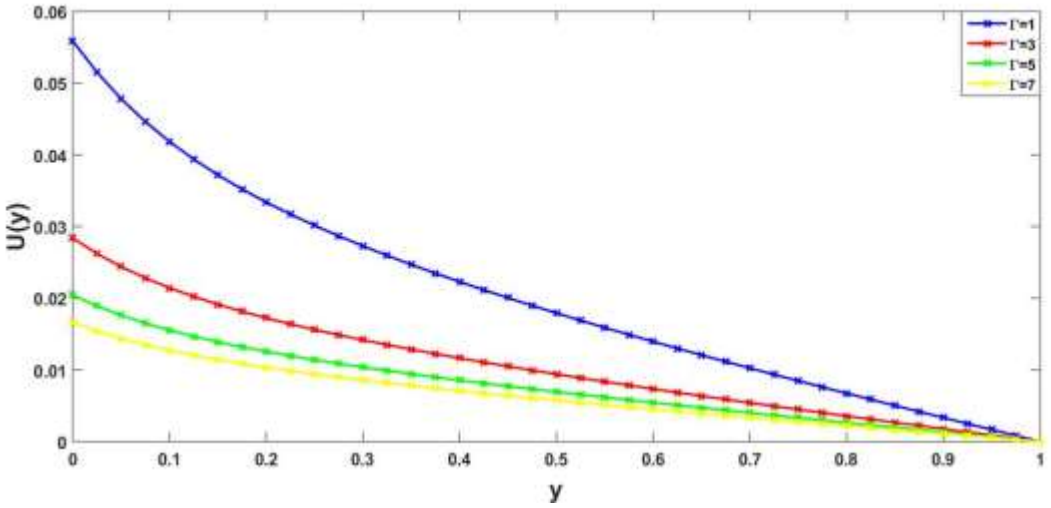

Figure 5: Velocity Changes for Concentration jump Parameter

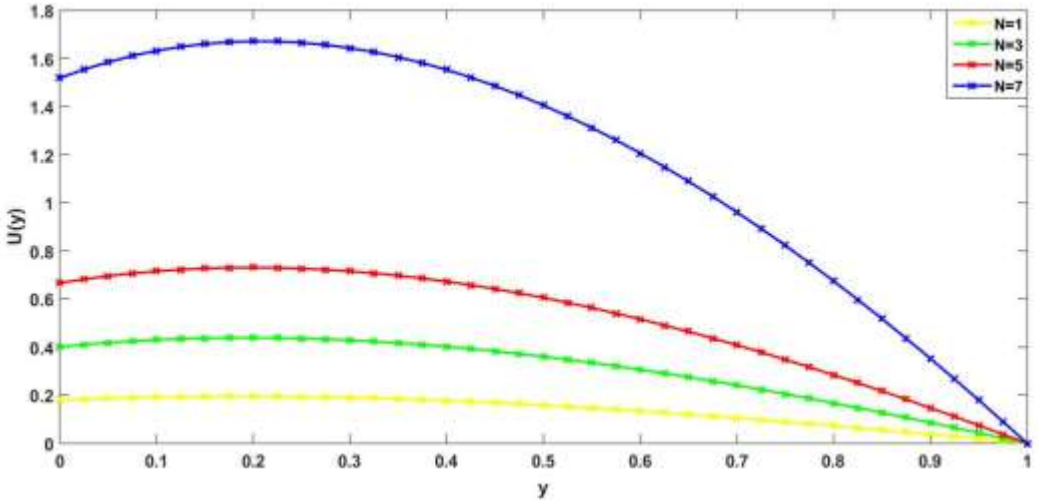

Figure 6: Velocity Changes for Sustentation Parameter

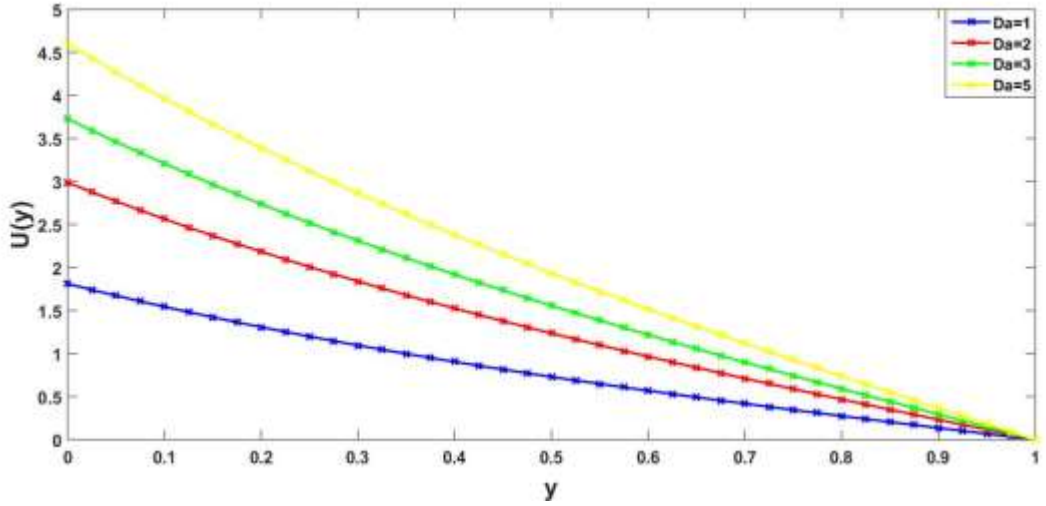

Figure 7: Velocity Changes for Darcy Porous Parameter

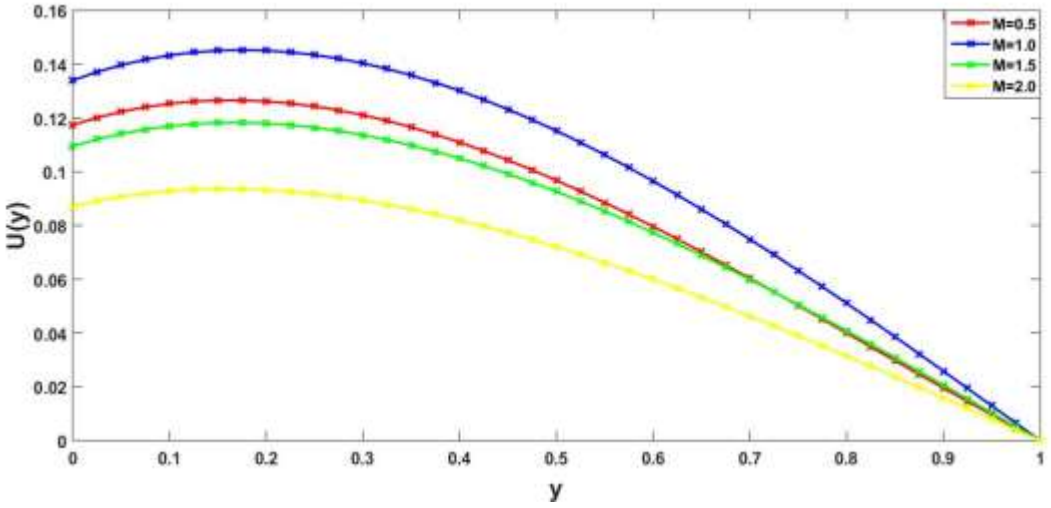

Figure 8: Velocity Changes for Magnetic Parameter

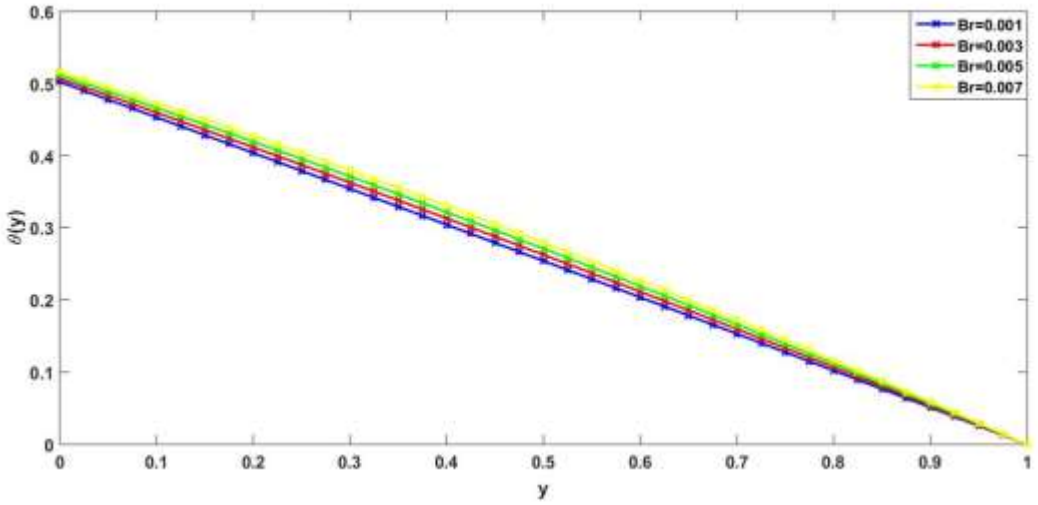

Figure 9: Temperature Changes for Brickman Parameter

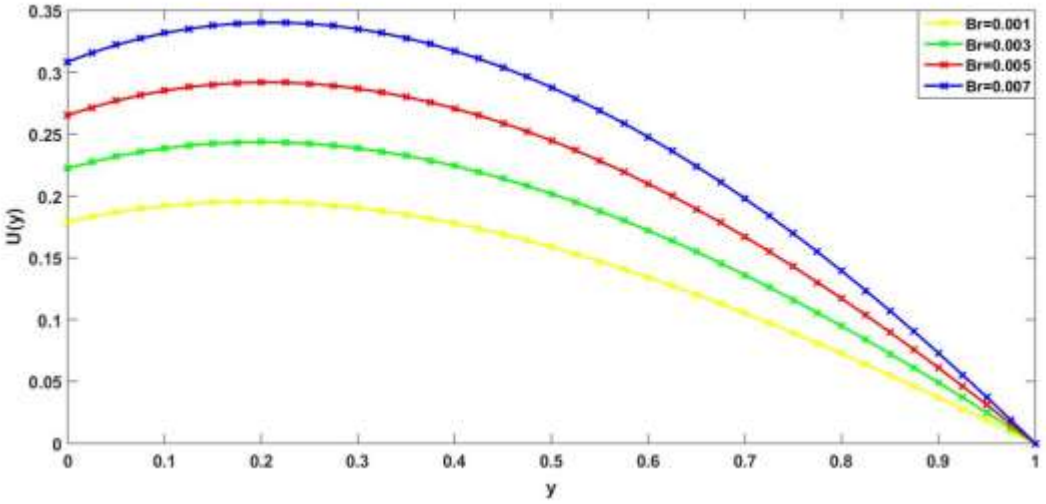

Figure 10: Velocity Changes for Brickman Parameter

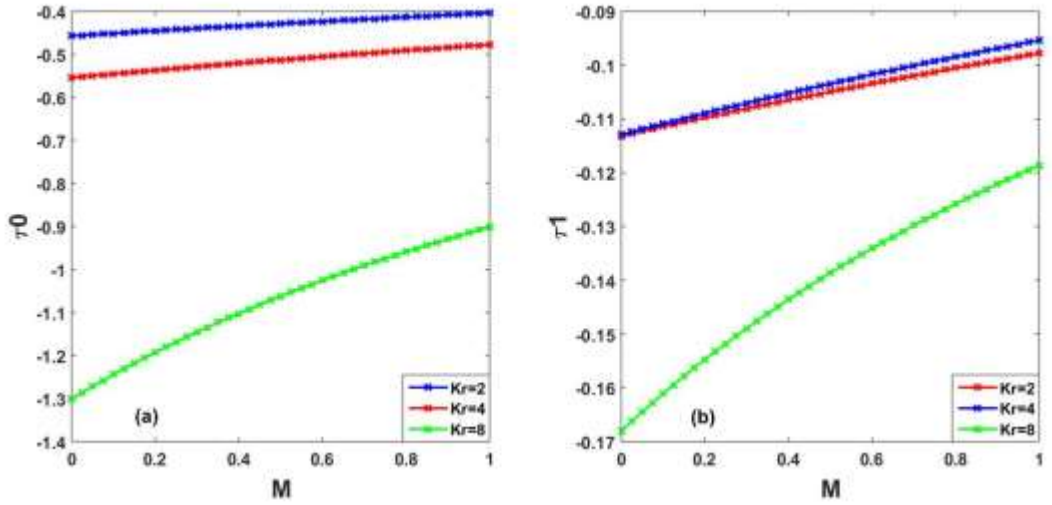

Figure 11: Skin friction Changes for Chemical Reaction Parameter

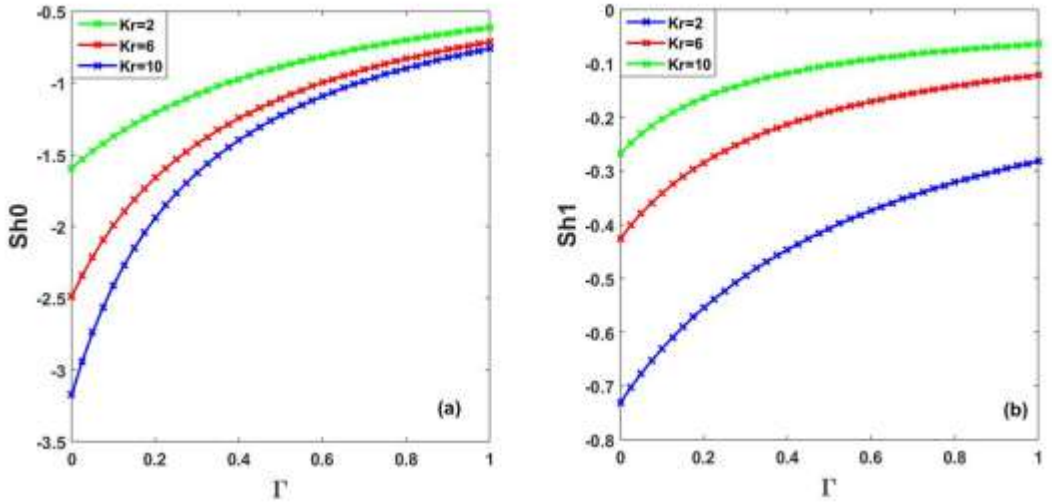

Figure 12: Sherwood Number Changes for Chemical Reaction Parameter

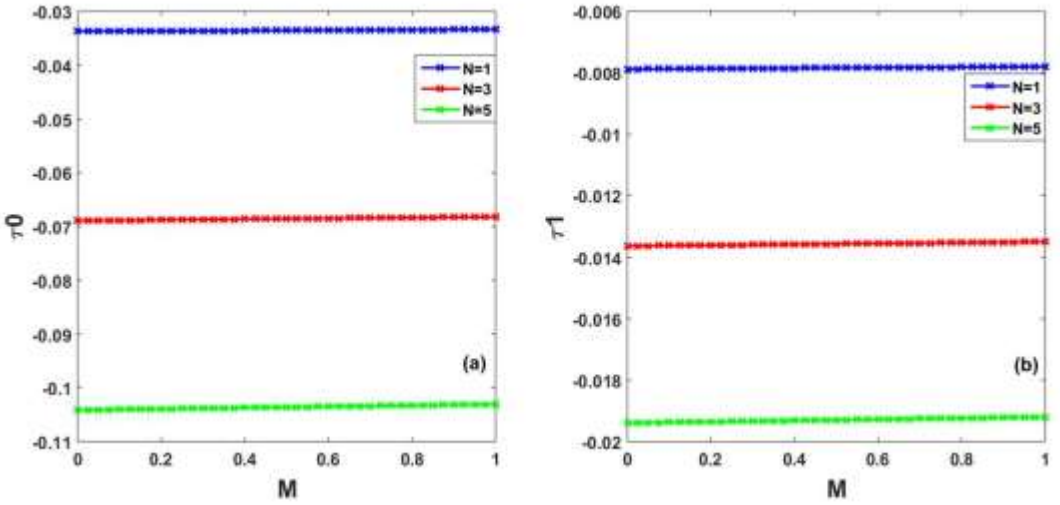

Figure 13: Skin friction Changes for Sustentation Parameter

4.1 Validation of Results

Table 1: Describes the numerical comparison between the work of Ojemeri and Onwubuya (2023) and the present work for constant values of other parameters.

The work of Ojemeri and Onwubuya (2023) is successfully recovered when $K_r = N = \Gamma = 0$

Y	Ojemeri and Onwubuya (2023) $\mathbf{M= 0.5, Da = 0.1, Br = 0.001}$ $\boldsymbol{\gamma = \lambda = 1}$		Present work $\mathbf{M= 0.5, Da = 0.1,}$ $\mathbf{Br = 0.001,}$ $\boldsymbol{\gamma = \lambda = 1}$ $\boldsymbol{K_r = N = \Gamma = 0}$	
	θ (Y)	U(Y)	θ (Y)	U(Y)
0.1	0.4500	0.0843	0.4500	0.0843
0.2	0.4000	0.0856	0.4000	0.0856
0.3	0.3500	0.0831	0.3500	0.0831
0.4	0.3000	0.0772	0.3000	0.0772
0.5	0.2500	0.0686	0.2500	0.0686

5.0 CONCLUSION

Coupling a chemical reaction with viscous dissipation in a superhydrophobic microchannel substantially regulates heat transfer and flow performance. The slip characteristics of the superhydrophobic surface amplify these thermal and momentum changes. These dynamics help optimize high-temperature engineering systems, such as combustion chambers, chemical reactors, and micro-scale cooling devices. The main summary from this research is highlighted as follows:

i. An increase in the chemical reaction parameter reduces the species concentration. The fluid consumes the diffusing chemical species faster, causing the concentration boundary layer to become thinner.

ii. The consumption of species and the dampening of concentration gradients lead to a negative acceleration or retardation of fluid motion, decreasing momentum transport and reducing skin friction at the boundary.

iii. Viscous dissipation turns the kinetic energy of the fluid motion into internal thermal energy. Higher viscous dissipation increases both fluid temperature and velocity.

iv. Slip velocity and temperature jump conditions at the superhydrophobic wall reduce flow resistance. This enhances velocity and thermal profiles more prominently near the treated wall compared to regular no-slip surfaces.

v. A stronger magnetic field creates a Lorentz force that slows down fluid motion, whereas a porous medium (represented by Darcy's number) increases fluid velocity.

vi. As the destructive chemical reaction parameter increases, the mass transfer rate at the walls intensifies, leading to an increase in the Sherwood number**.**

vii. The present mathematical model can be extended to consider the effect of thermal diffusion

REFERENCES

Ajibade, A. O. and Ojeagbase, P. O. (2020). Steady Natural Convection Heat and Mass Transfer Flow through a Vertical Porous Channel with Variable Viscosity and Thermal Conductivity, Engineering Reports, https://doi.org/10.1002/eng2.12268 2(11):12268.

Ajibade, A. O. and Umar, A. M. (2016). Effect of chemical reaction and radiation absorption on the unsteady MHD free convection Couette flow in a vertical channel filled with porous materials. Afr. Mat. 27, 201–213.

Bafakeeh O. T., Raza A., Khan U. S., Khan M. I., Nasr A., Khedher N.B. and Tag-Eldin E.M. (2022). Physical interpretation of Nanofluid (Copper Oxide and Silver) with slip and mixed convection effects: Application of fractional derivatives; *Applied Sciences*, 12 (21), 10860.

Dagana, J. and Amos, E. (2020). MHD Free Convection Heat and Mass Transfer Flow in a Porous Medium with Dufour and Chemical Reaction Effects, Int. J. Inno. Scientific & Eng. Tech. Res., 8(2):1-12.

Hamza M. M., Ochiba A. M., Muhammad I., and Akpootu D. O. (2026). Impact of suction/injection on convection-radiation flow in a superhydrophobic microchannel with viscous dissipation, *Journal of Mathematical Sciences and Computational Mathematics (JMSCM),* 7(1), 43-62.

Hamza, M. M., Shehu, A., Muhammad, I., Shuaibu, A., Ojemeri, G. (2024a). Electro-kinetically free convective heat flow in a slit microchannel, *International Journal of Applied and Computational Mathematics,* 10, https://doi.org/10.1007/s40819-024-01765-x

Hamza, M. M., Shehu, A., Muhammad, I., Shuaibu, A., Ojemeri, G. (2024b). Electrokinetically controlled mixed convective heat flow in a slit microchannel, *Heat Transfer,* DOI:10.1002/htj.23104

Heidarian, A., Rafee, R., Valipour, M. S. (2020). Effects of wall hydrophobicity on the thermohydraulic performance of the microchannels with nanofluids, *Int. Comm. Heat and Mass Transfer,* 117, https://doi.org/10.1016/j.icheatmasstransfer.2020.104758

Ibrahim M. and Ojemeri G. (2026). Influence of Jeffrey fluid on a magnetohydrodynamic (MHD) flow in a superhydrophobic microchannel affected by viscous dissipation, *Journal of Mathematical*

Sciences and Computational Mathematics (JMSCM), 7(2), pp. 223-240. DOI: doi.org/10.15864/jmscm/7202.

Ibrahim, F., Elaiw, A. and Bakr, A. (2008). Effect of the chemical reaction and radiation absorption on the unsteady MHD free convection flow past a semi-infinite vertical permeable moving plate with heat source and suction. Commun. Nonlinear Sci. Numer. Simul., 13, 1056–1066.

Jha, B. K. and Gwandu, B. J. (2018). MHD free convection flow in a vertical slit micro-channel with super- hydrophobic slip and temperature jump: Heating by constant wall temperature, *Alexandria Engineering Journal,* 57, https://dx.doi.org/10.1016/j.aej.2017.08.022.

Jha, B. K., Aina, B., and Ajiya, A. T. (2014). MHD natural convection flow in a vertical parallel plate microchannel, *Ain Shaums Engineering Journal,* **6**, pp. 289-295.

Kaita, I. H., Zayyanu, S. Y., Mas'ud, L., Hamsiu, A., Abdullahi, U. and Auwal, D. M. (2024). Heat and mass transfer flow in a channel filled with porous medium in the presence of variable thermal conductivity, 8(2), pp. 225 – 234.

Kesavaiah, D. C., Satyanarayana, P., and Venkataramana, S. (2011). Effects of the chemical reaction and radiation absorption on an unsteady MHD convective heat and mass transfer flow past a semi-infinite vertical permeable moving plate embedded in a porous medium with heat source and suction. Int. J. Appl. Math. Mech., 7, 52–69.

Makinde, O. D. (2010). On MHD Heat and Mass Transfer over a Moving Vertical Plate with a Convective Surface Boundary Condition, The Canadian Journal of Chemical Engineering, 88(6):983-990. https://doi.org/10.1002/cjce.20369.

Muthucumaraswamy, R. (2002). Effects of a chemical reaction on a moving isothermal vertical surface with suction. Acta Mech, 155, 65–70.

Ojemeri G. and Onwubuya I. O. (2023). Significance of Viscous Dissipation and Porosity Effects in a Heated Superhydrophobic Microchannel, *Journal of Engineering and Technology (JET)*, 14(2), pp. 287-305.

Ojemeri, G., Onwubuya I. O., Omokhuale, E., Hussaini A. and Shuaibu, A. (2024). Analytical investigation of Arrhenius kinetics with heat source/sink impacts along a heated superhydrophobic microchannel, *UMYU Scientifica,* 3(1), 61-71. DOI:105619/usci.2431.004.

Omokhuale E. and Ojemeri G. (2025). Arrhenius-controlled fluid flow over a superhydrophobic microchannel with symmetric wall concentration, Journal of Basic Physical Research, 14(1), pp. 77 – 90. https://journals.unizik.edu.ng/jbpr/

Omokhuale E., Godwin Ojemeri G., Alechenu B., Germache H. I., and Dazi J. A. (2025). Dynamical Behaviour of Wall Concentration and Superhydrophobicity Effects on a Combined Reactive Flow in a Slit Microchannel, International Journal of Science for Global Sustainability, 11(3), 41-51. doi: https://doi.org/10.57233/ijsgs.v11i3.918.

Raghunath, K. and Obulesu, M. (2022a). Unsteady MHD oscillatory Casson fluid flow past an inclined vertical porous plate in the presence of chemical reaction with heat absorption and Soret effects. Heat Transf., 51, 733–752.

Raghunath, K., Nagesh, G., Reddy, V. R. C. and Obulesu, M. (2021). Unsteady MHD fluid flow past an inclined vertical porous plate in the presence of chemical reaction with aligned magnetic field, radiation, and Soret effects. Heat Transf., 51, 2742–2760.

Raghunath, K., Obulesu, M., Sujatha, S., and Venkateswaraju, K (2022b). Investigation of MHD Casson fluid flow past a vertical porous plate under the influence of thermal diffusion and chemical reaction. Heat Transf. 2022, 51, 377–394.

Reddy, V. R., Raghunath, K. and Obulesu, M. (2022). Characteristics of MHD Casson fluid past an inclined vertical porous plate. Mater. Today Proc., 49, 2136–2142.

Rout, B. R., Parida, S. K. and Panda, S. (2013). MHD Heat and Mass Transfer of Chemical Reaction Fluid Flow over a Moving Vertical Plate in Presence of Heat Source with Convective Surface Boundary Condition, International Journal of Chemical Engineering, 1:1-10. https://doi.org/10.1155/2013/296834

Saeed, U. J., Sami, H., Inayat, S. A. and Ilyas, K. (2019). Heat and Mass Transfer of Free Convection Flow over a Vertical Plate with Chemical Reaction under Wall Slip Effect, Arabian Journal for Science and Engineering, 44:9869-9887. https://doi.org/10.1007/s13369-019-03863-1

Sehra, S., Sami, H., Inayat, S. A. S., Saeed, U. J., Ilyas, K. and Nisar, K. S. (2021). Convection Heat Mass Transfer and MHD Flow over a Vertical Plate with Chemical Reaction, Arbitrary Shear Stress and Exponential Heating, Scientific Reports, 11:4265. https://doi.org/10.1038/s41598-021 81615-8.

Sharma, H., Gaddam, A., Agrawal, A., Joshi, S.S. and Dimov, S. S. (2020). Influence of texture shape and arrangement on thermo-hydraulic performance of textured microchannels, *Int. J. Therm. Sci.*, 147, https://doi.org/10.1016/j.ijthermalsci.2019.106146.

Sia, G. D., Lim, C.S., Tan, M.K., Chen, G.M. and Hung, Y. M. (2023). Anomalously enhanced subcooled flow boiling in superhydrophobic graphene-nanoplatelet-coated microchannels, *Int. Comm. Heat and Mass Transfer,* 146, https://doi.org/10.1016/j.icheatmasstransfer.2023.106932.

Yale I. D., Uchiri A. M. T., Hamza M. M., and Ojemeri G. (2023). Effect of viscous dissipation fluid in a slit microchannel with heated superhydrophobic surface, *Dutse Journal of Pure and Applied Sciences,* 9(3b), pp. 290-302.

Zhang, W., Wang, Q., Zeng, M., and Zhao, C. (2019). Thermoelectric effect and temperature-gradient-driven electrokinetic flow of electrolyte solutions in charged nanocapillaries. *International Journal of Heat and Mass Transfer, 143, https://*doi:10.1016/j.ijheatmasstransfer.2019.118569.